Contents lists available at ScienceDirect

BBA - Molecular Cell Research

journal homepage: www.elsevier.com/locate/bbamcr

The bacterial magnesium transporter MgtA reveals highly selective interaction with specific cardiolipin species

Julia Weikum [a,b], Jeroen F. van Dyck [c], Saranya Subramani [a], David P. Klebl [d], Merete Storflor [e], Stephen P. Muench [d], Sören Abel [e], Frank Sobott [c,f,*], J. Preben Morth [a,b,g,**]

[a] Membrane Transport Group, Centre for Molecular Medicine Norway (NCMM), Nordic EMBL Partnership, University of Oslo, P.O. Box 1137, Blindern, 0318 Oslo, Norway
[b] Enzyme and Protein Chemistry, Section for Protein Chemistry and Enzyme Technology, Department of Biotechnology and Biomedicine, Technical University of Denmark, Søltofts Plads, 2800 Kgs. Lyngby, Denmark
[c] Department of Chemistry, University of Antwerp, Campus Groenenborger, Groenenborgerlaan 171, G.V. 418, 2020 Antwerpen, Belgium
[d] School of Biomedical Sciences & The Astbury Centre for Structural Molecular Biology, University of Leeds, Woodhouse Lane, Leeds LS2 9JT, United Kingdom
[e] Infections Biology Lab, Department of Pharmacy, UiT-The Arctic University of Norway, 9037 Tromsø, Norway
[f] School of Molecular and Cellular Biology & The Astbury Centre for Structural Molecular Biology, University of Leeds, Woodhouse Lane, Leeds LS2 9JT, United Kingdom
[g] Institute for Experimental Medical Research (IEMR), Oslo University Hospital, Ullevål PB 4956 Nydalen, NO-0424 Oslo, Norway

A B S T R A C T

The bacterial magnesium transporter A (MgtA) is a specialized P-type ATPase important for Mg^{2+} import into the cytoplasm; disrupted magnesium homeostasis is linked to intrinsic ribosome instability and antibacterial resistance in *Salmonella* strains. Here, we show that MgtA has functional specificity for cardiolipin 18:1. Still, it reaches maximum activity only in combination with cardiolipin 16:0, equivalent to the major components of native cardiolipin found in *E. coli* membranes. Native mass spectrometry indicates the presence of two binding sites for cardiolipin, agreeing with the kinetic studies revealing that a cooperative relationship likely exists between the two cardiolipin variants. This is the first experimental evidence of cooperative effects between lipids of the same class, with only minor variations in their acyl chain composition, acting on a membrane protein. In summary, our results reveal that MgtA exhibits a highly complex interaction with one cardiolipin 18:1 and one cardiolipin 16:0, affecting protein activity and stability, contributing to our understanding of the particular interactions between lipid environment and membrane proteins. Further, a better understanding of Mg^{2+} homeostasis in bacteria, due to its role as a virulence regulator, will provide further insights into the regulation and mechanism of bacterial infections.

1. Introduction

Biological membranes function as a dynamic interplay between proteins and lipids. The plasma membrane contains a specific lipid composition that can differ locally, and these regions can accommodate functional specialization based on non-random lipid-lipid and lipid-protein interactions [1]. The lipid ensemble reveals a high degree of molecular variation in the head group structure. It presents various functional groups at the membrane surface and in the acyl chains, with their variable length and degree of saturation [2], located within the transmembrane segment. This combinatorial space opens the possibility of an additional regulatory function by lipids of the same type, which differ only marginally in their acyl chain composition but have unique

structural and functional properties [3]. Significant progress has been made in elucidating the intricate and complex interplay between membrane proteins and lipids from experimental studies [3–6], or several P-type ATPase family members, a role of specific lipid interactions have been elucidated, specifically the plasma membrane Ca^{2+}-ATPase (PMCA). Dimyristoyl phosphatidylcholine interactions cause differences in activity between PMCA2 and PMCA4 [7], and lipid binding stoichiometries were found to depend on the functional state of the PMCA [7]. The prominent Na^+/K^+-ATPase is strongly stimulated and inhibited by lipid-protein interactions [8]; of particular importance is the modulatory effect of cholesterol [9] and the stimulatory effect of polyunsaturated lipids such as phosphatidylethanolamine (PE) and phosphatidylserine (PS) [8,10]. The stimulus mainly accelerates the

E1P–E2P conformational transition and is mediated by two independent lipid binding sites, with a PS lipid bound between αTM8–10 and the FXYD transmembrane helix and a PE bound between αM2, 4, 6, and 9 [11].

Membrane proteins from bacterial species have also been investigated, and while many, however not all, show selective lipid binding [5], their functional role often remains poorly understood. Typically, structural studies have revealed the molecular basis of various lipid binding sites in membrane proteins. Specific binding pockets for lipids are referred to as «non-annular lipid sites,» characterized by longer lipid residence times [6,12]. They are stabilized through polar interactions between head groups and charged amino acids at the water-lipid interface or hydrophobic interactions between acyl chains and hydrophobic residues in the transmembrane segments [6,12]. Interestingly, the lipid composition of the membrane, which determines the bulk properties of the lipid bilayer, such as membrane fluidity and bilayer thickness, also influences membrane protein function, as shown for certain P-type ATPases [13]. Lipids that associate weakly with transmembrane segments exhibit faster lipid exchange rates. They have been termed «annular lipids/annular lipid shells» as they often form a ring-like structure around the membrane-embedded protein section [12]. This study mainly focuses on non-annular, i.e., tightly bound and structural lipids, in particular interactions between MgtA and specific cardiolipin species.

The magnesium transporter A (MgtA) is a primary active Mg^{2+} transporter, transporting Mg^{2+} from the periplasm to the cytoplasm with orthology widely distributed throughout eubacteria, fungi, and plants [14,15]. The transporter ensures Mg^{2+} homeostasis, essential for stabilizing membranes and ribosomes, ensuring correct folding of oligonucleotides, and functions as a co-factor for enzymatic reactions. Additionally, Mg^{2+} has been revealed as a bacterial virulence regulator [16] and can also protect against hostile environments, such as withstanding nitro-oxidative stress in professional phagocytes during infection [17]. Furthermore, a recently discovered role for MgtA, especially its homolog MgtB, suggests that the transporters promote survival in macrophages during infections by preventing Mg^{2+} deprivation [18].

MgtA is a P-type ATPase transporter that utilizes energy from the hydrolysis of adenosine triphosphate (ATP) for Mg^{2+} transport [16,19] and exhibits a classical P-type ATPase structural composition with three cytoplasmic domains, termed nucleotide-binding (N), phosphorylation (P) and actuator (A) domain, and a transmembrane core with ten transmembrane helices [20]. The expression of MgtA is tightly regulated by the two-component system PhoP/PhoQ, which upregulates MgtA levels under low extracellular Mg^{2+} concentrations, low pH, and in the presence of antibacterial peptides [16]. The PhoP/PhoQ-induced sigma factor RpoS accumulates as a response to low cytoplasmic Mg^{2+} levels, tied to the presence of functional Mg^{2+} homeostasis mediated via MgtA and MgtB in *Salmonella* and other pathogens [21–23]. Additional regulation of MgtA expression is present through the *mgtA* mRNA leader region, *mgtL*, which senses intracellular Mg^{2+} levels and only promotes MgtA translation under low intracellular Mg^{2+} concentrations [24–26]. The enzymatic activity of MgtA is also under tight regulation through substrate inhibition by Mg^{2+}_{free}, which allows MgtA activation only in the concentration range of 10 μM to 1 mM Mg^{2+}_{free} [15]. Mg^{2+}_{free} describes Mg^{2+} ions that are not coordinated by ATP but are available for transport by MgtA. However, the mechanism of MgtA inhibition by Mg^{2+}_{free} remains unclear. While most of our understanding of bacterial Mg^{2+} homeostasis derives from *Salmonella*, considerable similarities between *E. coli*, which only has MgtA and not its homolog MgtB, have been described [27].

MgtA is located in the inner membrane of *E. coli*, which contains only approximately ~5 % cardiolipin (CL), with the remainder being ~75 % phosphatidylethanolamine (PE) and ~ 20 % phosphatidylglycerol (PG) [28]. Previously, we have shown that CL performs an essential function for MgtA activation and that it co-localizes at the inner membrane of *E. coli* poles and septal regions [15]. Cardiolipin has four acyl chains compared to classical glycerophospholipids, which only have two. In contrast to eukaryotes, which often have only one or two major cardiolipins [29], *E. coli* contains a large variety of CL species with variable hydrophobic tails with palmitic acid (16:0), palmitoleic acid (16:1) and oleic acid (18:1) as the most abundant acyl chains [30]. It has been proposed previously that the anionic head group of cardiolipin is most critical for MgtA ATPase activity. At the same time, the acyl chain composition of the lipid only contributes marginally to the enzyme activation [15]. Therefore, a function of cardiolipin as a Mg^{2+} or H^+ chaperone or reservoir for MgtA-mediated Mg^{2+}-transport was hypothesized [15]. The data presented here, however, indicates a more complex interaction between MgtA and cardiolipin. This study shows the specific interaction of MgtA with selected cardiolipin species. Enzyme kinetics studies and native mass spectrometry determined that these lipid-protein interactions are likely mediated through site-specific interactions and biophysical properties of the lipid bilayer environment. We reveal high selectivity of MgtA for CL species 18:1 and CL 16:0 and cooperativity of binding these two CL molecules to MgtA.

Additionally, we show thermal stabilization of MgtA by CL 18:1 through nano differential scanning fluorimetry, while no effect on MgtA stabilization by CL 16:0 was detected. These results highlight the complexity of lipid-membrane protein interactions, with highly selective roles found even for closely related lipid species varying only slightly in acyl chain structure. The implications of this exquisite fine tuning of membrane protein function might suggest a much more significant role in lipid composition than previously anticipated.

2. Material and methods

Lipids were purchased from Avanti Polar Lipids and solubilized in chloroform. *E. coli* cardiolipin (cat no. 841199), cardiolipin 18:1 (cat no. 710335), and cardiolipin 16:0 (cat no. 710333) were purchased as stock solutions of 10 mg/ml. Cardiolipin 14:1 (cat no. 710337) and 16:1 (cat no. 710339) were obtained as stock solutions of 5 mg/ml. Total *E. coli* lipid extract (cat no. 100500) and 1-palmitoyl-2-oleoyl-sn-glycero-3-phosphoethanolamine (POPE) (cat no. 850757) were purchased as 25 mg/ml stock solution. Detergents were obtained from either Chemical Point UG, Deisenhofen, Germany, for n-dodecyl-β-D-maltopyranoside (DDM) or from Nikko Chemicals for octaethylene glycol monododecyl ether ($C_{12}E_8$). All other chemicals were purchased as grade BioUltra from Sigma-Aldrich.

2.1. Heterologous expression and purification of MgtA

Cloning of *E. coli* MgtA into pETM11 vector (EMBL), heterologous expression in *E. coli* C43(DE3), and purification were performed as previously described [15,31]. In brief, isolated *E coli* membranes with overexpressed MgtA were solubilized in 1 % β-dodecyl maltoside (β-DDM) prior to Histrap HP (GE Healthcare) purification equilibrated in 25 mM HEPES pH 7.0, 100 mM K_2SO_4, 5 % glycerol, 1 mM PMSF, 5 mM β-mercaptoethanol, 3× CMC β-DDM, and eluted in 25 mM HEPES pH 7.0, 100 mM K_2SO_4, 5 % glycerol, 1 mM PMSF, 5 mM β-mercaptoethanol, 300 mM imidazole pH 7.6. The elution was followed by size exclusion chromatography using a HiLoad 16/600 Superdex 200 pg column equilibrated with 1.5 CV of buffer E (25 mM HEPES, pH 7.0, 100 mM K_2SO_4, 5 % glycerol, 1 mM dithiothreitol, 3× CMC β-DDM).

2.2. ATPase enzymatic assay

Lipid stocks for ATPase enzymatic assays were prepared by tempering indicated lipids, dissolved in chloroform, to room temperature, or heating them to 40 °C until completely dissolved. The lipids were dried under an argon stream with vigorous shaking. The dried lipid film was resuspended in Milli-Q water and 20 mM $C_{12}E_8$ with vigorous shaking for at least 1 h at RT and sonication intervals of 5–10 min in between. A lipid stock concentration of 6.12 mM or 12.24 mM for lipid

profiles or 12 mM for Mg^{2+} profiles, respectively, was obtained. Fresh lipid stocks were prepared prior to enzymatic assays. For enzymatic assays in the presence of increasing lipid concentrations (lipid profiles), dilutions to indicated concentrations were prepared in Milli-Q water with 20 mM $C_{12}E_8$. The same volume (1 μl) of lipid dilutions was added to the reaction volume to keep detergent levels constant (final concentration: $3\times$ CMC $C_{12}E_8$), independent of the lipid concentration.

ATPase enzymatic assays measuring ATP hydrolysis by detecting released inorganic phosphate were performed according to the protocol described earlier [15]. The online web service MAXC (maxchelator.stanford.edu) was used to calculate Mg^{2+}_{free} levels in the presence of given concentrations of ATP at pH 7.0 at 37 °C. Apparent V_{max} and K_m were calculated by fitting the curves (specific activity) as a function of Mg^{2+}_{free} using a modified uncompetitive substrate inhibition model (Eq. (1))

$$Y = \frac{V_{max}X}{K_m + X\left(1 + \frac{X^n}{K_i}\right)} \tag{1}$$

with X referring to the substrate concentration, Y to the enzyme activity and n to the number of uncompetitive inhibitor sites, provided by GraphPad Prism8 (www.graphpad.com). k_{cat} was estimated using the formula $k_{cat} = V_{max}/[MgtA]$.

The Hill coefficient for CL activation was obtained by fitting the curves using the allosteric sigmoidal Eq. (2)

$$Y = \frac{V_{max}X^h}{K_{half}^h + X^h} \tag{2}$$

provided by GraphPad Prism8, with X referring to the substrate concentration, Y to the enzyme activity, K_{half} to the substrate concentration that produces half-maximal enzyme velocity, and h to the Hill slope.

2.3. Native mass spectrometry

Native mass spectrometry (native MS) was performed on purified MgtA protein and subsequently incubated with lipids depending on the experiment. For lipid selectivity of MgtA, total *E. coli* lipid extract (consisting of 67 % PE, 23 % PG, and 10 % CL) was used, while selected lipids, POPE and CL, were included for competition assays. Chloroform, in which lipids were dissolved, was removed under an argon stream until the lipid film was completely dry. The lipid film was resuspended in buffer (25 mM HEPES, pH 7.0; 200 mM KCl; 5 % Glycerol) and $6\times$ CMC (1.02 mM) DDM for a final concentration of 1.47 mg/ml for total *E. coli* lipid (for lipid selectivity) or 400 μM for CL and 2.4 mM for POPE (for competition assays). For the competition assays, CL and POPE were mixed in the indicated ratio. MgtA was diluted in the buffer to a final concentration of 20 μM. 25 μl MgtA (20 μM) were mixed with 25 μl lipid solution and incubated for 16 h at 4 °C in a rotator (5 rpm).

MgtA protein samples had to be desalted prior to the native MS measurement. This was accomplished by washing the sample several times in a 100 kDa cut-off concentrator column, with the cut-off small enough to remove most of the unbound lipids and protein-free detergent micelles as well as the non-volatile salts. The protein micelle mass was expected to be around 170 kDa (102.5 kDa for MgtA + ca. 65–70 kDa for the DDM micelle). MgtA was washed with freshly prepared aqueous ammonium acetate (AmAc) at a concentration of 200 mM (adjusted with ammonium hydroxide to pH 7.0), including $3\times$ CMC DDM or $C_{12}E_8$. 25 μl MgtA was added to 475 μl washing solution in the cut-off concentrator column. The sample was concentrated back to 25 μl (ca. 20 μM protein, without Mg added) by spinning it at 10,000 g at 4 °C. When concentrated, the flow-through was discarded, and 475 μl fresh wash solution was added. Wash steps were repeated four times, after which the sample was placed in an Eppendorf tube on ice until measurement.

This procedure, called detergent wash, removes bound lipids and replaces them with detergent. The desalting and buffer exchange to ammonium acetate (e.g., 100 mM) is a standard procedure required for native MS, both for soluble and membrane proteins, and well established to preserve native interactions and folds. No SEC analysis was performed after the detergent wash to check whether the protein remains intact.

Native MS measurements were performed with a Synapt G2 HD Q-TOF mass spectrometer (Waters, Wilmslow, UK; apart from Supplementary fig. 3 where a Synapt G1 was used; see figure legend) with traveling wave (T-wave) ion mobility, using nano-electrospray ionization (ESI) with gold-coated borosilicate capillaries prepared in-house. Instrument parameters in TOF mode were chosen to preserve non-covalent interactions while ensuring optimum spectral resolution: capillary voltage 2.0 kV; source temperature 30 °C; sampling cone 150–200 V; extraction cone 2.0 V; trap collision energy 150 V; transfer collision energy 125–150 V; trap DC bias 2 V. Gas pressures in the instrument were: source 6.4 mbar; trap cell 2.0–2.8×10^{-2} mbar; transfer cell 2.5×10^{-2} mbar; IM cell 3.7×10^{-4} mbar. Settings were optimized to provide desolvated ions while maintaining important noncovalent interactions.

2.4. Nano differential scanning fluorometry (nanoDSF)

E. coli cardiolipin, specific cardiolipin species, or POPE dissolved in chloroform were dried under an argon stream. The lipid film was resuspended in buffer (25 mM HEPES, pH 7.0; 200 mM KCl; 5 % glycerol and $21\times$ CMC (1.9 mM) $C_{12}E_8$) to a final concentration of 1.3 mM. MgtA (final concentration: 14 μM) was mixed with lipid in a 1:100 M ratio in a final detergent concentration of $3\times$ CMC $C_{12}E_8$ and filled up with buffer to 40 μl sample volume. Samples were incubated at 4 °C for 16 h, and afterward, excess lipids were removed by centrifugation (20,000 g, 15 min, 4 °C). nanoDSF was performed using Prometheus NT.48 (Nanotemper) in a temperature range of 15–95 °C with a temperature gradient of 1 °C per minute. A minimum of triplicates was used for all experiments.

Protein melting temperatures were determined as maxima of the first derivative of the 350 nm/330 nm ratio determined by GraphPad Prism8 (www.graphpad.com).

2.5. In vivo localization

A plasmid carrying clo*ver-mgtA* was created by gene synthesis (Eurofin Genomics). A start codon free *mgtA* was connected to the 3′ end of a stop codon free *clover* by a linker (GGATCCGCTGGCTCCGCTGCTGGTTCTGGCGAATTCggatatc). The sequence is a Gly and Ser rich, flexible linker previously designed for GFP fusions [32].

This construct was inserted behind the P_{araBAD} promoter of pBAD33.1 (pBAD33.1 was a gift from Christian Raetz; Addgene plasmid #36267; http://n2t.net/addgene:36267; RRID: Addgene_36267) [33], so that the ATG of the *Nde*I restriction site in pBAD33.1 is replaced by the clover start codon to create pSoA280. pSoA280 was transformed in *E. coli* MG1655, MG1655 *clsABC*::FRT (MG1655 Δ*cls*; PO10), and *Vibrio cholerae* c6706. All bacteria were grown at 37 °C in Luria-Bertani (LB) medium with aeration. The media were supplemented with 50 μg/ml or 5 μg/ml chloramphenicol for *E. coli* or *V. cholerae*, respectively, to maintain the plasmid. Clover-MgtA fusion proteins were expressed by adding 0.2 % L-arabinose (Sigma) in the exponential growth phase for 2 h. A Deltavision Elite (GE Healthcare) microscope equipped with Deltavision CMOS camera, a climate chamber set to 37 °C, and a UPlanFLN $100\times$ PH NA1.30 objective (Olympus) was used to image bacteria. 2 μl induced bacterial culture was spotted on a 1 % agar patches immediately prior to microscopy and images in the phase contrast as well as the GFP channel were acquired. The software Oufti (2015 Oufti, Jacobs-Wagner Lab) was used to detect bacteria in the phase contrast channel and overlay their outlines with a mesh that subdivides each cell into segments [34]. This mesh was used to quantify the fluorescent intensity in each subdivision in the GFP channel. Intensity values and cell lengths were extracted from the Oufti output files using Matlab (R2019a,

Mathworks) and used to plot the intensity profiles of cells. For better visualization, the microscopic images were adjusted using the levels tool in Photoshop CS6 (Adobe) by setting the same black- and white-point values for all fluorescent images.

2.6. SDS-PAGE and immunoblot

A total of 20 ml LB supplemented with appropriate concentrations of arabinose and chloramphenicol were inoculated 1:100 with overnight culture. Cultures were grown for 2 h at 37 °C with aeration. The OD_{600} of the culture was measured, and similar cell amounts were harvested by centrifugation at ~20000 x*g* at 4 °C. Pellets were resuspended in SDS loading buffer (50 mM Tris-HCl (pH 6.8); 2 % sodium dodecyl sulfate (SDS); 100 mM dithiothreitol (DTT); 10 % glycerol, 0.02 % NaN_3) and heated for 10 min at 90 °C. The samples were separated by SDS-polyacrylamide gel electrophoresis (PAGE) on 10 % gels and transferred to nitrocellulose membranes (BioRad). Clover was detected using monoclonal antibodies (anti-GFP 1:5000, Santa Cruz Biotechnologies) and monoclonal anti mouse secondary antibodies conjugated to horseradish peroxidase (1:5000, Bio-Rad). After incubation with ECL substrate (BioRad), chemiluminescence was recorded on a Bio-Rad ChemiDoc MP Imaging System.

2.7. Flow cytometry

A volume of 5 ml LB, supplemented with appropriate concentrations of arabinose and chloramphenicol, was inoculated 1:100 with overnight culture. Cultures were grown for 2 h at 37 °C with aeration. The OD_{600} of the culture was measured, and the same amount of cells was harvested by centrifugation at 20000 x*g* at 4 °C. Pellets were resuspended in PBS and FSC, SSC, and fluorescence (EX 488 nm; EM 533 ±30 nm) were rescored on a BD Accuri C6 Plus Flow Cytometer (BD Biosciences). PBS was used as a control to distinguish bacterial cells from other particles in FSC and SSC.

3. Results

3.1. Native mass spectrometry reveals the selective binding of two putative cardiolipin molecules

Native mass spectrometry (MS) has recently emerged as a powerful tool for investigating dynamic and heterogeneous membrane protein structures and lipid interactions [35,36]. This approach was used in this study to characterize the stoichiometry of MgtA-lipid interactions, and to investigate the selectivity of specific cardiolipin species binding preferentially to the protein.

m/z difference		
	22+	21+
MgtA >MgtA + 1x CL	62.54 ± 7.35	66.17 ± 10.83
MgtA + 1x CL >MgtA + 2x CL	65.32 ± 5.03	68.88 ± 6.97

mass difference (Da)		
	22+	21+
MgtA >MgtA + 1x CL	1375 ± 161	1389 ± 238
MgtA + 1x CL >MgtA + 2x CL	1437 ± 105	1446 ± 146
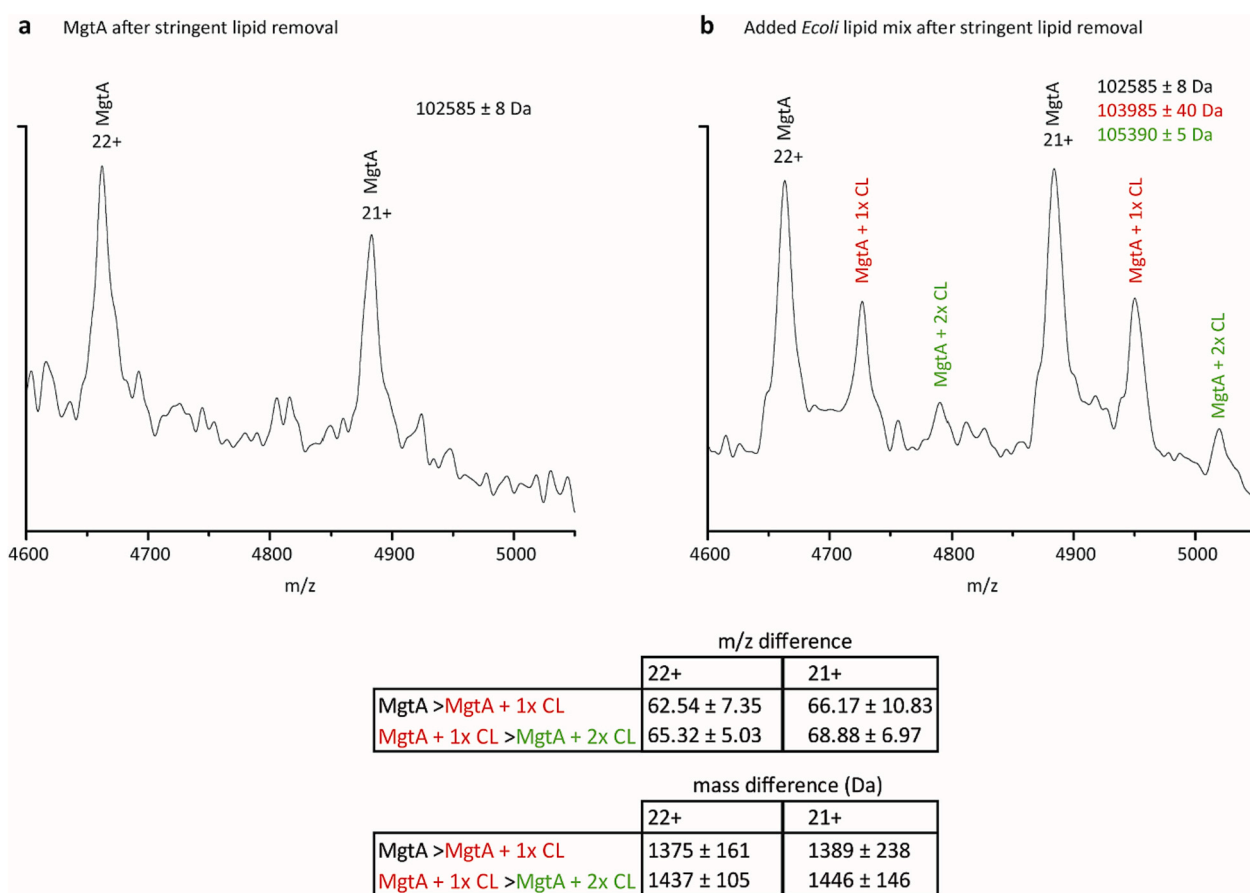
Fig. 1. MgtA shows selective binding of cardiolipin in native mass spectrometry.
Purified MgtA solubilized in 3× CMC DDM was analyzed by native MS (a) in the absence or (b) presence of total *E. coli* lipid extract. Total *E. coli* lipid extract contains only 9.8 % CL, while the remaining lipids are 57.5 % PE, 15.1 % PG and 17.6 % unknown (Avanti Polar Lipids). The left spectrum shows the most intense charge states 22+ and 21+ of purified MgtA after lipid removal by high CMC DDM. The right spectrum exhibits MgtA as seen after incubation with *E. coli* lipid mixture. This sample was washed with 3× CMC DDM to remove weakly bound lipids leaving only the strongest interacting lipids. The spectrum on the right reveals additions of approximately 1400 and 2800 Da (red and green) which correspond to the molecular weight of one and two cardiolipin molecules, respectively. The spectra were recorded in TOF mode and the key MS settings are the voltages (sampling cone, trap collision, transfer collision and trap bias) and pressures (backing pressure, trap cell pressure). These values were 200 V, 150 V, 150 V, 2 V, 6.4 mbar and 1.97×10^{-2} mbar respectively. (For interpretation of the references to colour in this figure legend, the reader is referred to the web version of this article.)

Lipid interaction experiments were performed on purified protein, but full delipidation was not always achieved with the protocol (described in Material and Methods), with some samples showing low levels of retained native lipids. Two types of experiments were carried out: (i) a full *E. coli* lipid extract (Avanti Polar Lipids) was added to the purified protein in the presence of 3× CMC DDM in order to examine lipid binding selectivity, and (ii) a titration with cardiolipin (CL) was carried out to investigate binding affinity, using POPE as a nonspecific binding control. The *E. coli* lipid extract (Avanti Polar Lipids) used for MgtA lipidation contains only 9.8 % CL, while the majority of the lipids are PE (57.5 %), PG (15.1 %) and uncharacterized components (17.6 %). Cardiolipin used for titration experiments was extracted from *E. coli* membranes (Avanti Polar Lipids), containing a large variety of CL species with different acyl chain compositions.

Fig. 1a shows two charge states (*m/z* peaks) in the native mass spectrum of delipidated MgtA in the absence of Mg^{2+} and ATP (as purified) and without the addition of lipids; the corresponding full mass spectrum is shown in Supplementary Fig. 1. From this, the protein mass is determined experimentally as 102,585 +/− 8 Da, which matches the calculated sequence mass for MgtA, i.e. 102,665.0 Da with and 102,533.8 Da without the N-terminal methionine, reasonably well. Fig. 1b shows the same charge states, using the same experimental conditions also in the absence of Mg^{2+} and ATP, after incubation of purified MgtA with *E. coli* lipid extract and subsequent detergent wash. Additional peaks are apparent now, which suggests that lipid binding is detected, with the apparent mass shift for the first binding event calculated from these charge states as ca. 1380 +/− 200 Da, and for the second as ca. 1440 +/− 125 Da. These masses broadly correspond to the molecular weight of one and two cardiolipin molecules, respectively. It should be noted that other lipids present in the extract, in particular, PE (719.3 Da) and PG (761.07 Da), have masses which are roughly half the mass of CL. It is, therefore, possible, at the limited mass resolution obtained on this instrument, that the observed lipid adduct peaks might be instead due to two or four bound PE or PG molecules, respectively. However, in that case the mass spectra would also be expected to show the 1× and 3× bound states, which is not the case. The identification of the bound lipids as cardiolipin species is also further corroborated by the following data.

We additionally performed a competition experiment in which the binding of cardiolipin was studied in the presence of another lipid, POPE, added in large excess (Fig. 2 and Supplementary Fig. 2). POPE is a major lipid component present in the *E. coli* membrane and, therefore, was used as a negative control representing the native *E. coli* lipid environment. Additionally, POPE was included to evaluate if hydrophobic exposed patches on the protein show any nonspecific lipid interactions in our setting. Lipid binding to MgtA was studied in the absence and presence of CL with increasing concentrations up to 30 μM, and correspondingly decreasing concentrations of POPE from 1000 to 970 μM, respectively. This leaves the total lipid concentration constant at 1000 μM, which corresponds to a 1:100 M ratio between MgtA and lipid. In this experiment, samples were obtained from a different protein batch, and even the control sample (first two panels in Fig. 2a, Purified MgtA after lipid removal, and 1000 μM POPE) revealed already a low amount of bound cardiolipin, which was most likely retained during the purification process in this case. These co-purified cardiolipins were not observed in the delipidated sample of the previous experiment (Fig. 1), presumably due to differences in delipidation efficiency. Nevertheless, the addition of increasing amounts of CL showed a corresponding increase in the relative intensity of adduct peaks, which correlate to those seen in Fig. 1, with the relative intensity of the 1× bound state in particular increasing slightly from ca. 25 % to ca. 30 %, for both the 25+ and 24+ charge states. Interestingly, the 2× lipid-bound peak intensity does not change significantly within the limited concentration range studied here (Fig. 2b and Supplementary Fig. 2). While the data demonstrate qualitatively that the binding of the first CL lipid occurs with higher affinity and increases with increasing CL concentration, the

second lipid binding event is of lower affinity and can only be seen clearly above 20 μM CL (i.e., at a 2:1 ratio to the protein).

These results support that MgtA selectively binds up to two cardiolipin molecules and not any other lipids present in the native *E. coli* membrane. They also show that the first binding event happens with higher affinity, and the mass of this cardiolipin species appears to be somewhat lower than that of the second one binding, although the achievable mass resolution and peak shapes do ultimately not allow to make firm conclusions. With a more powerful spectrometer, the masses of the individual lipids bound could be determined more accurately, and the lipid titration series presented here could also be extended to higher CL:POPE ratios in order to quantitatively determine binding affinities and possible cooperative effects.

3.2. No specificity of cardiolipin binding to selected conformational states of MgtA was detected

As a P-type ATPase, MgtA transports Mg^{2+} according to the catalytic cycle described by the Post-Albers-scheme [35]. During the catalytic cycle, MgtA likely alternates between different conformational states, as described in the introduction for the Na^+/K^+-ATPase. The two major conformational states are termed E1 and E2, which exhibit large structural differences and different affinities to the transported ion and counter ion [35] (Supplementary Fig. 3A). To investigate whether MgtA has a higher affinity for cardiolipin in one specific conformational state, which would indicate a role of cardiolipin for a specific transport step, the protein was incubated with inhibitors AlF_4^- and $ADP-AlF_4^-$. These inhibitors essentially mimic phosphate and ATP at the binding sites on the enzyme and lock MgtA in the two different conformational states, E1 and E2, respectively. Both AlF_4^- and $ADP-AlF_4^-$ have previously been shown to inhibit the MgtA from *E. coli* [15]. We expect $ADP-AlF_4^-$ to stabilize the E1 state, occluding protons, even though it is yet not established whether MgtA does export protons, and the AlF_4^- is expected to stabilize the E2 state, occluding Mg ions. This would be similar to other P-type ATPases such as the Na^+, K^+-ATPase [37] and the Gastric H^+, K^+ -ATPase [38], able to trap two K^+ ions in the occluded E2-Pi state mimicked by AlF_3. The ATP11C flippase is locked in both E2-Pi and E2P states in the presence of AlF alone [39]. After samples were incubated with inhibitors, CL extracted from the *E. coli* membrane (*E. coli* CL) was added to MgtA as previously described. Native MS spectra showed similar binding of cardiolipin in all samples (Supplementary Fig. 3B). This indicates that there is no, or only a minimal, preference for cardiolipin to a selected conformational state of MgtA. In summary, we find that MgtA contains two specific binding sites for lipids and selectively binds cardiolipin, among other major lipids present in *E. coli* membranes.

3.3. The composition of the hydrophobic cardiolipin tail plays a major role in MgtA activation

Cardiolipins are anionic lipids with a unique dimeric structure, with two phosphate ester groups and four acyl chains (Fig. 3A). While the head group defines the lipid class, large molecular diversity is present through variations in the length and saturation degree of the fatty acid chains (Fig. 3A). Previously, we have shown that cardiolipin is required for MgtA activation [15]. However, all enzymatic assays were performed in the presence of cardiolipin extracted from *E. coli* membranes consisting of a mixture of different cardiolipin species [15]. To investigate whether specific cardiolipins stimulate MgtA activity, cardiolipin species with varying acyl chain length and saturation were used in the ATPase assay. In *E. coli,* a large variety of cardiolipin species have been detected, with over 50 different types present ranging in acyl carbon chain length from 12 to 19 containing different acyl chain combinations [30]. Commercially, only cardiolipins with four identical acyl chains are available at Avanti Polar Lipids, whereas the most common natural cardiolipins in the *E. coli* membrane contain mixed acyl chains. We used
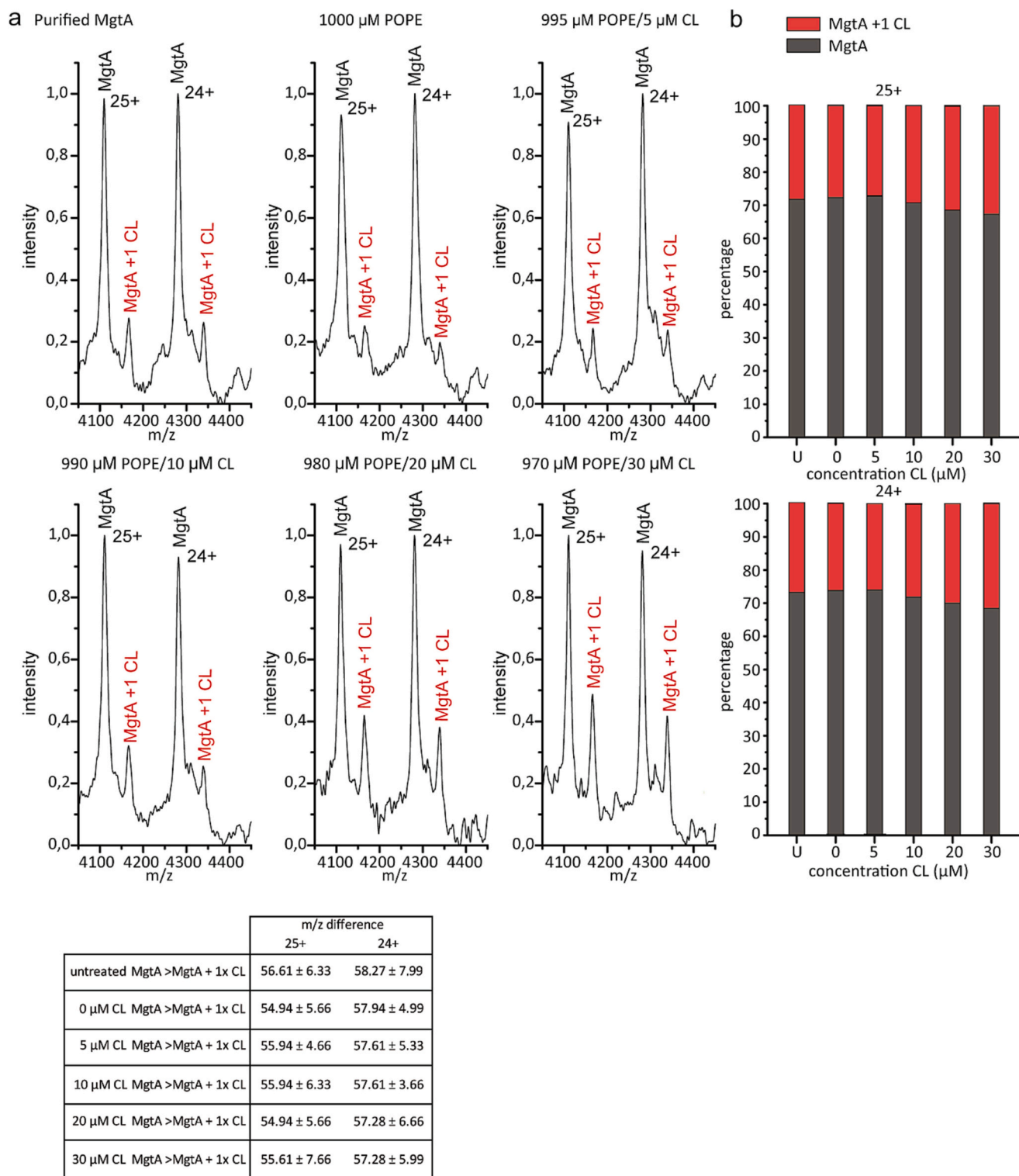
Fig. 2. Cardiolipin competition assay of MgtA in the presence of POPE reveals increase in CL binding.

a) MS spectra showing a lipid competition assay of MgtA with increasing CL concentrations (0 to 30 μM) and 1000 to 970 μM POPE. In the spectra 1× and 2× CL adducts are assigned. In b) the increase in 1× or 2× CL molecules bound to MgtA is shown as percentages according to the increase in CL added to the sample. The spectra were recorded in TOF mode and the key MS settings are the voltages: sampling cone, trap collision, transfer collision, trap bias and pressures: backing pressure, trap cell pressure. These values where 150 V, 150 V, 125 V, 2 V, 8.4 mbar and 2.8×10^{-2} mbar. The table shows the m/z difference for both charged states 24+ and 25+, with the addition of 1 or 2 CL.
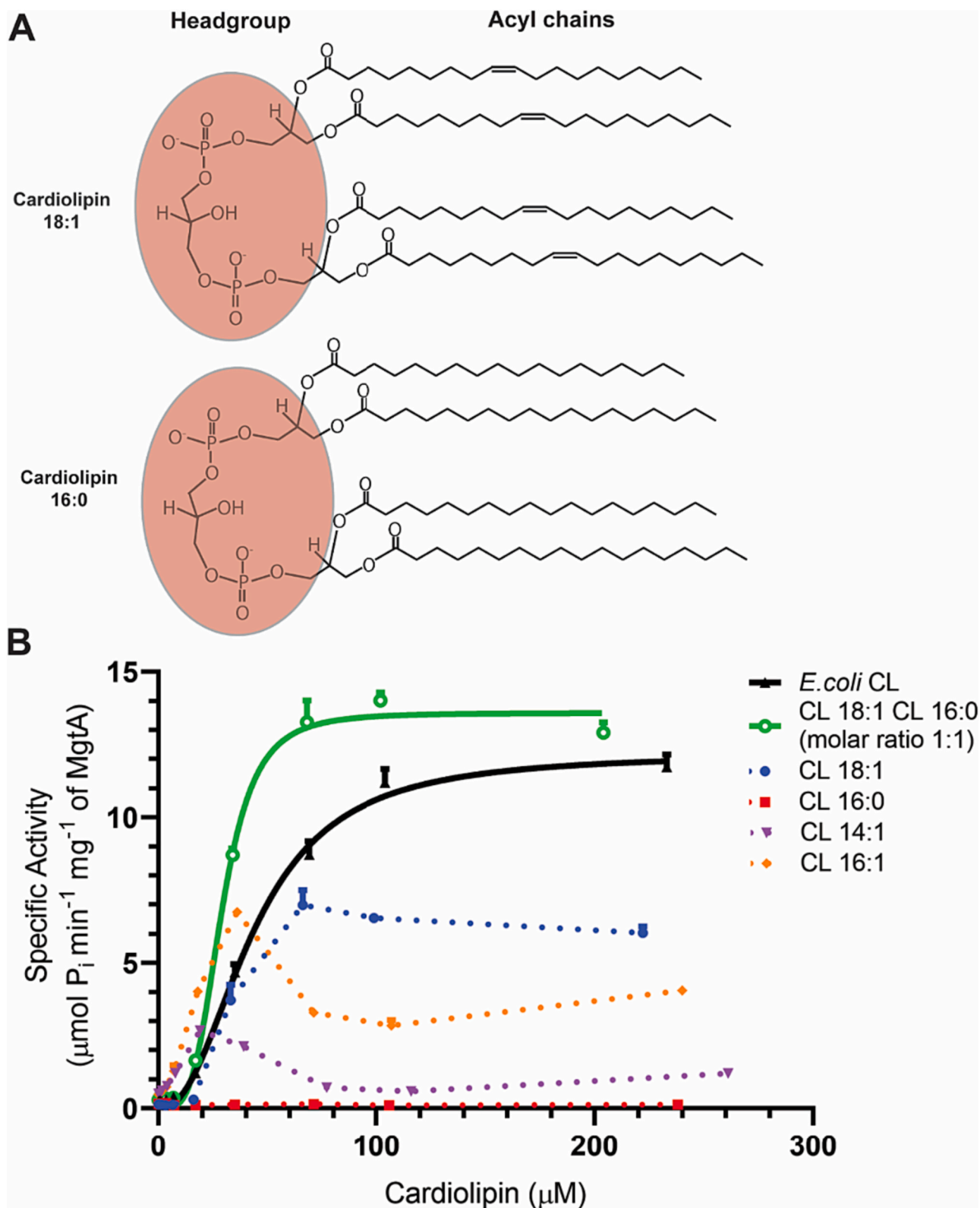
Fig. 3. *E. coli* MgtA shows cooperative binding of specific cardiolipin species.

(A) Cardiolipins 18:1 and 16:0 contain the same polar hydrophilic headgroup (red) but exhibit differences in the length and saturation degree of their acyl chains. (B) Concentration-dependent activation of MgtA ATPase activity by *E. coli* extracted cardiolipin (black), a 1:1 mixture of cardiolipin 18:1 and 16:0 (green) or individual cardiolipin species. Lipids are prepared as described in the Material and methods section; specific activity is determined by measuring phosphate release. Curves are representatives from three independent experiments, showing mean $+/-$ SD. Enzymatic activation curves were fitted to an allosteric sigmoidal model (GraphPad, Prism8). Fitting curves are shown (lines) for data with least squares fit of 0.95 or above with parameters described in Table 1. The dotted lines represent activation curves that could not be fitted with the allosteric sigmoidal model. (For interpretation of the references to colour in this figure legend, the reader is referred to the web version of this article.)

the CL species with the most common acyl chains in *E. coli*, i.e., palmitic acid (16:0), palmitoleic acid (16:1), and oleic acid (18:1). Large differences in MgtA ATPase activity levels were detected in the presence of these different types of cardiolipin molecules (Fig. 3B). For instance, activity was reduced to approximately 50 % in the presence of CL 18:1 and to barely 10 % in the presence of CL 14:1 in comparison to *E. coli* CL. In the presence of any single cardiolipin species, MgtA activity never reached the same activation level as in the presence of *E. coli* extracted cardiolipin.

Interestingly, an equimolar combination of two species, CL 18:1 and 16:0, exhibited higher MgtA ATPase activity levels relative to *E. coli* CL at the same protein: lipid ratio. It is noteworthy that although MgtA shows lower activity in the presence of CL 18:1 alone, CL 16:0 by itself does not seem to activate MgtA at all. This corresponds to previous results comparing MgtA activation in the presence of cardiolipin extracted from either *E. coli* or bovine heart membranes, which showed a decreased activity in the latter [15]. While cardiolipins share the same head group, *E. coli* cardiolipin has a diverse fatty acid composition with 16:0–18:1 fatty acids at positions 1 and 2 of sn-glycerol 3-phosphate as the most dominant species (35 %). In contrast, bovine heart CLs contain almost entirely linoleate chains (18:1, 18:2, 18:3) and no stearic chains (16:0) [15].

As activity studies shown in Fig. 3B revealed the importance of two different cardiolipin species, 18:1 and 16:0, for MgtA activity, we hypothesized the specific interactions of these two lipid species with individual binding sites in MgtA. ATPase activity in the presence of selected cardiolipin species followed a sigmoidal shaped curve, which indicates cooperative binding at more than one binding site (Fig. 3B). Cooperativity in protein-ligand interaction refers to increased affinity for additional ligands upon binding of the first ligand in the case of positive cooperativity or decreased ligand affinity of the protein for additional ligands for negative cooperativity [40]. The cooperativity of ligand binding can be quantified by the Hill coefficient (n_H), which measures the sigmoidal character of the activation curve [41]. The reference state is a hyperbolic curve with a single monomeric binding site characterized by $n_H = 1$. Therefore, binding curves with $n_H > 1$ are a direct measurement of cooperativity. Although n_H is not a direct measurement of ligand binding sites, it is a useful index for the theoretical upper limit of the number of binding events [41]. Only recently, the first case of allosteric modulation and positive cooperativity of lipid binding has been detected for *E. coli* ammonium channel AmtB [42]. Fitting the cardiolipin-dependent activation curve of MgtA to a sigmoidal allosteric model revealed positive cooperativity of cardiolipin binding (Fig. 3B; Table 1). In our analysis, only the least square fits (R-square) of 0.95 or above were considered, i.e., only activation curves in the presence of *E. coli* CL and the 18:1 / 16:0 mixture in equimolar ratio. MgtA activation curves in the presence of CLs 14:1, 18:1, 16:1, and 16:0 were excluded based on the poorer fit. Plotting of MgtA activation curves in the presence of *E. coli* CL, or equimolar amounts of CL 18:1 and 16:0, against an allosteric sigmoidal fit showed a Hill coefficient of 2.4–3. This supports the hypothesis of more than one cardiolipin binding site with cooperative binding of multiple CL species.

3.4. Cardiolipin 16:0 is required for optimal MgtA activation

To better understand the effect of CL 18:1 and 16:0 and their

Table 1
Allosteric fit of purified MgtA in the presence of different cardiolipin species. The V_{max} and Hill coefficient were determined by the least squares fit of the data from Fig. 1B, as described in materials and methods. Only data from least squares fit of 0.95 or above was included in the analysis.

	V_{max} (µmol min^{-1} mg^{-1})	Hill coefficient
E. coli CL	11.0 +/− 0.8	2.4 +/− 0.6
CL 18:1 / 16:0 (molar ratio 1:1)	14.1 +/− 1.9	3.0 +/− 0.8

combination on MgtA activation, ATPase activity profiles in the presence of these CL species with increasing Mg^{2+} concentrations were performed. The total lipid concentration was kept constant at 200 µM in all experiments. Results confirmed previous observations that equimolar amounts of both lipid species lead to maximum activation (Fig. 4A), mimicking the activity levels achieved previously in the presence of native *E. coli* CL (14). In the presence of CL 18:1 alone, MgtA exhibited lower levels of activity, while no measurable ATPase activity was observed in the presence of CL 16:0 alone (Fig. 4A). To assess how the molar ratio between CL 18:1 and 16:0 affects activation levels, ATPase assays were performed with molar ratios of 3:1 and 1:3, with either CL 18:1 or 16:0 as the major lipid. Additionally, a molar ratio of 1:1 between CL 18:1 and 16:0 (as above) was included again. Maximum enzyme activity was obtained only when 50 % or more of the lipid content consisted of CL 16:0. Enzymatic assays with higher percentages of CL 18:1, e.g., in the 3:1 ratio, resembled the activity levels obtained in the presence of CL 18:1 alone (Fig. 4B).

To verify whether only either CL 18:1 or 16:0, mixed with another cardiolipin species, were needed for optimal activation, ATPase assays in the presence of CL 18:1 or 16:0 mixed in a 1:1 M ratio with CL 16:1 were performed (Fig. 4C). Activation levels did not reach their maximum for samples containing CL 16:1 alone or in combination with CL 16:0 or 18:1. This highlights the importance of both species, CL 18:1 and 16:0, for MgtA activation. It should be noted, though, that only activating effects according to cardiolipin species were investigated, whereas possible variations in binding affinities between cardiolipin species were not assessed. As all experiments were, however, performed in large excess of CL at the same total concentration of 200 µM, we assume that if CL 16:0 would exhibit a much higher binding affinity than CL 18:1, it would occupy both binding sites, even in a sample with the majority of lipid represented by CL 18:1, and therefore MgtA would exhibit similar activity levels as in samples containing CL 18:1 and 16:0 in a 3:1 and 1:1 M ratio.

Calculated V_{max}, K_m, and k_{cat} in the presence of different cardiolipin species are given in Table 2. Interestingly, higher V_{max} and k_{cat} values were observed in the presence of CL 18:1 and 16:0 in equimolar amounts (V_{max}: 19.3 µmol min^{-1} mg^{-1}, k_{cat}: 32.8 s^{-1}) or in excess of CL 16:0 (V_{max}: 24.6 µmol min^{-1} mg^{-1}, k_{cat}: 41.8 s^{-1}) in comparison to previously obtained kinetic parameters in the presence of *E. coli* CL (V_{max}: 13.7 µmol min^{-1} mg^{-1}, k_{cat}: 23 s^{-1}) [15]. However, K_m values also increased for both samples (CL 18:1/16:0 1:1, 67 µM; CL 18:1/16:0 3:1, 120.9 µM) in comparison to *E. coli* CL (10 µM), indicating decreased affinity for Mg^{2+}_{free}. It should be noted that K_m increased for all samples containing CL 16:0 or 16:1. Overall, results indicate an intricate interplay of lipid species CL 18:1 and 16:0 for maximum activity of MgtA.

3.5. MgtA reveals increased thermal stability in the presence of specific cardiolipin species

To determine the effect of cardiolipin on MgtA thermal stability, nano differential scanning fluorimetry (nanoDSF) was performed in the presence of *E. coli* CL or POPE in a 1:100 protein-lipid molar ratio, matching native MS experiments (Fig. 5A). Melting temperatures revealed an increase of ca. 7 °C in the presence of *E. coli* CL (T_m: 49.7 °C) relative to purified MgtA without lipids. The presence of POPE (T_m: 42.2 °C) did not show any upward temperature shift and resembled the control of MgtA without lipids (T_m: 41.8 °C) (Table 3). This indicates that cardiolipin specifically stabilizes MgtA, while the presence of any other lipid environment, represented by POPE as a major *E. coli* lipid component, does not lead to significant protein stabilization. To analyze whether specific cardiolipin species affect MgtA stability differently, nanoDSF was performed with CL 18:1, 16:0, and mixtures of both in different ratios (Fig. 5B and C). In the presence of CL 18:1, the melting temperature of MgtA was significantly increased by ca. 10 °C, while no thermal stabilization was detectable in the presence of CL 16:0 alone (Fig. 5B). Melting curves in the presence of both CL 18:1 and 16:0
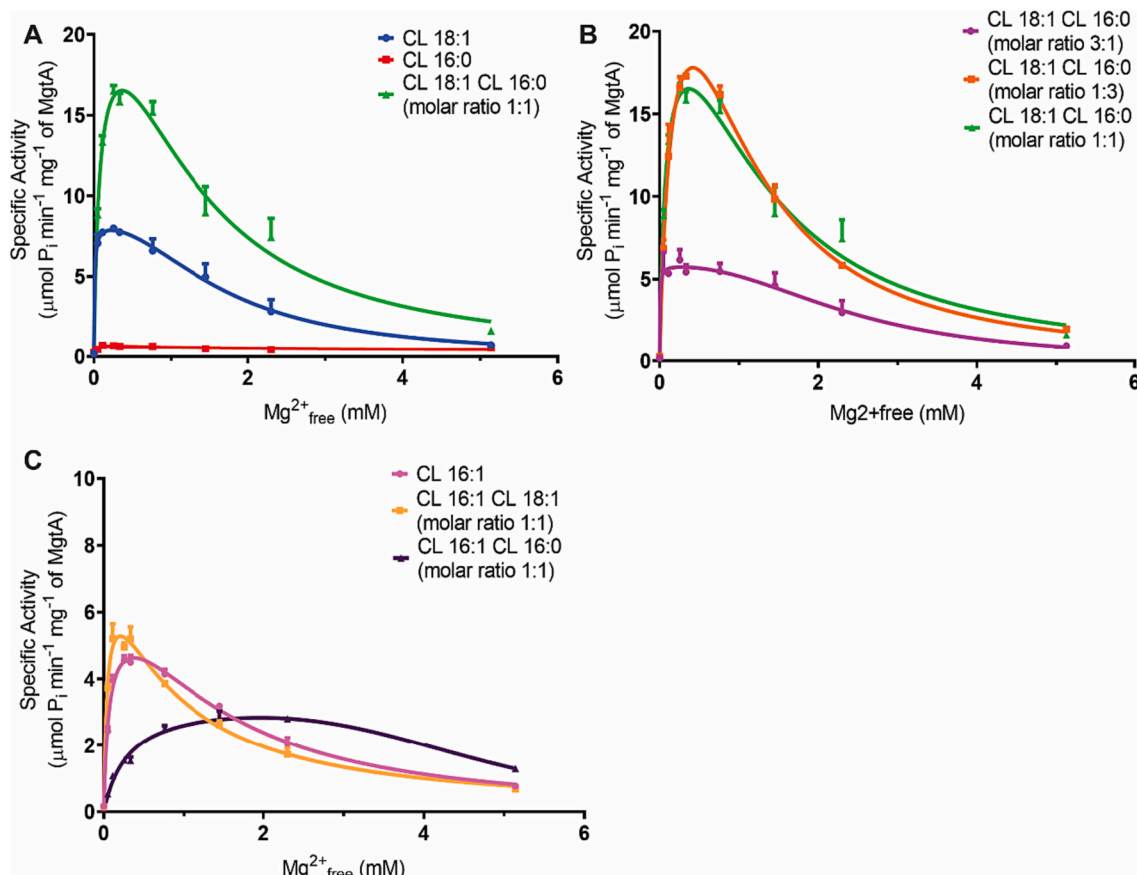
Fig. 4. *E. coli* MgtA shows selective activation by cardiolipin species 18:1 and 16:0 in specific molar ratios.
ATP hydrolysis was measured in the presence of specific cardiolipin species with increasing concentrations of Mg^{2+} at 3 mM ATP. Lipid concentration was kept constant at 200 μM (molar ratio of MgtA to lipid 1:5000). Curves are representatives from three independent experiments, showing mean +/− SD. Enzymatic data was fitted as a function of Mg^{2+}_{free} using the Michaelis-Menten equation (GraphPad Prism 8) as described in the Material and methods section. Kinetic parameters are described in Table 2. Mg^{2+}_{free} profiles of (A) CL 18:1, 16:0 and an equimolar mixture of both or (B) CL 18:1 and 16:0 in different molar ratios were assessed. (C) As a control Mg^{2+}_{free} profiles of CL 18:1 or 16:0 in combination with CL 16:1 were performed.

Table 2
Kinetic property of purified MgtA in the presence of different cardiolipin species. The apparent V_{max}, K_m, and turnover number (K_{cat}) values were determined by the least squares fit of the data from Fig. 2A, B, and C and put in references to previously obtained kinetics [15].

	V_{max} (μmol min^{-1} mg^{-1})	K_m (μM)	K_{cat} (s^{-1})
E. coli CL (Subramani et al. (2016))	13.7 +/− 0.2	10 +/− 0.6	23 +/− 0.3
CL 18:1	7.6 +/− 0.7	12 +/− 7.0	12.8 +/− 1.2
CL 16:0	N/A	N/A	N/A
CL 18:1 / 16:0 (ratio 1:1)	19.3 +/− 2.4	67 +/− 3.0	32.8 +/− 4.1
CL 18:1 / 16:0 (ratio 3:1)	7.1 +/− 0.9	4.4 +/− 2.6	12.06 +/− 1.5
CL 18:1 / 16:0 (ratio 1:3)	24.6 +/− 6.7	120.9 +/− 48.9	41.8 +/− 11.4
CL 16:1	6.0 +/− 0.5	103 +/− 5	10.2 +/− 0.8
CL 18:1 / 16:1 (ratio 1:1)	6.6 +/− 0.8	40 +/− 12	11.3 +/− 1.4
CL 16:0 / 16:1 (ratio 1:1)	3.9 +/− 0.5	285 +/− 44	6.7 +/− 0.8

revealed increased stabilization when a higher proportion of CL 18:1 was present in the mixture (Fig. 5C). While a 1:3 mixture with CL 16:0 as the major component or 1:1 CL 18:1/16:0 showed melting temperatures of 42.5 and 43.2 °C, respectively, in a 3:1 mixture with CL 18:1 as the

major component, a melting temperature of 47 °C was determined. This reflects previous results from the enzymatic studies, which revealed activation in the presence of CL 18:1 and 16:0, while in the presence of CL16:0 alone, no activity was detectable. Interestingly, the thermal stabilization of MgtA is noticeable in the presence of CL 18:1 alone, while this single cardiolipin species was not enough for maximal enzymatic activation.

As a control, thermal stabilization of MgtA in the presence of only the inhibitors, AlF_4^- and ADP-AlF_4^-, was investigated, which revealed no effect (Fig. 5D). It should be mentioned that melting curves in the presence of *E. coli* CL, CL 18:1, and 18:1/16:0 mix showed a flattened curve compared to the control without lipids. MgtA was incubated with the indicated lipids in excess overnight (1:100 M ratio between MgtA and lipid), and excess lipid was removed prior to the experiment by centrifugation. In the case of *E. coli* CL, CL 18:1 and 18:1/16:0, some of the protein was removed during the centrifugation step, likely pulled down together with the excess lipid. This affected the final protein concentration in the experiment. The different curve shapes might, therefore, be due to lower protein concentrations or due to the presence of lipid vesicles forming around the protein, which could interfere with the absorbance measured at 350 and 330 nm upon unfolding. Interestingly, the removal of protein by centrifugation of excess lipids already indicates the binding of MgtA to the *E. coli* CL and CL 18:1. In summary, MgtA is selectively stabilized by a specific cardiolipin species, CL 18:1.
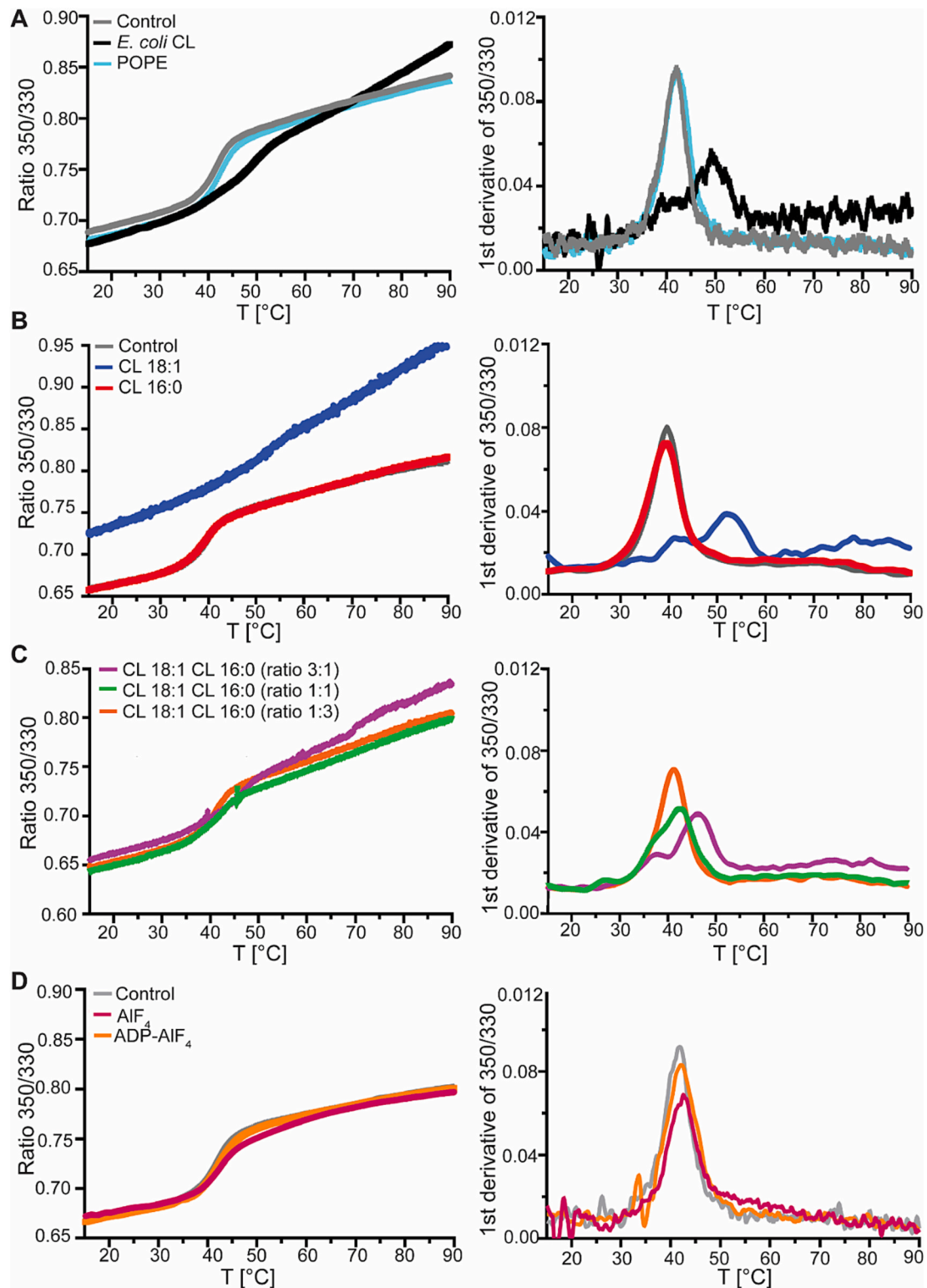
Fig. 5. MgtA shows increased temperature stabilization in the presence of the specific cardiolipin species, cardiolipin 18:1.
Nano differential scanning fluorimetry (nanoDSF) curves (left) and their first derivative (right) of purified MgtA in the presence of (A) cardiolipin and 1-Palmitoyl-2-oleoyl-sn-glycero-3-phosphoethanolamine (POPE) or specific cardiolipin species CL 18:1 and CL 16:0 (B) alone and (C) in different molar ratios were obtained. MgtA was incubated overnight with indicated lipids in a 1:100 M ratio, and samples were centrifuged to remove excess lipids. Melting curves were performed on Prometheus NT.48 (Nanotemper) in a temperature range of 15 °C – 95 °C and a temperature gradient of 1 °C per minute. A paired, one-sided *t*-test was applied. ***p < 0.001. (D) Additionally, melting curves were performed on MgtA in the presence of inhibitors ADP-AlF$_4^-$ and AlF$_4^-$. MgtA was incubated with inhibitors in a 1:500 M ratio (2.95 mM) for two hours at 4 °C before melting curves were performed. Curves are representatives from three independent experiments, showing mean +/− SD. Obtained melting temperatures are described in Table 3.

Table 3
Melting temperatures of MgtA in the presence of lipids and inhibitors determined by nanoDSF. Statistics were carried out using paired, one-sided t-test. ***$p < 0.001$.

	Melting temperature [°C]
MgtA (control)	41.8 +/− 0.4
MgtA in the presence of *E. coli* cardiolipin	49.7 +/− 1.4 ***
MgtA in the presence of POPE	42.2 +/− 0.4
MgtA in the presence of cardiolipin 18:1	52.5 +/− 1.2 ***
MgtA in the presence of cardiolipin 16:0	40.3 +/− 1.0
MgtA in the presence of cardiolipin 18:1 16:0 (molar ratio 3:1)	47.0 +/− 0.8
MgtA in the presence of cardiolipin 18:1 16:0 (molar ratio 1:1)	43.2 +/− 1.2
MgtA in the presence of cardiolipin 18:1 16:0 (molar ratio 1:3)	42.5 +/− 1.2
MgtA in the presence of AlF$_4^-$	41.8 +/− 0.6
MgtA in the presence of ADP-AlF$_4^-$	41.6 +/− 0.6

3.6. Cardiolipin is not the sole signal for the localization of MgtA to cell poles

Previously, we showed co-localization of a fluorescently-tagged MgtA to *E. coli* C43(DE3) cell poles [15]. As C43(DE3) is an expression strain with genetic modifications in comparison to wild type *E. coli* [43], we verified here that fluorescently-tagged MgtA under the arabinose promoter (Fig. 6A) also localizes to the cell poles in wild-type strain *E. coli* MG1655 (Fig. 6B). Additionally, we could detect the localization of MgtA to cell poles in cardiolipin-deficient strain MG1655Δ*cls* that contains a deletion of all three cardiolipin synthases (Fig. 6B). To test whether the cardiolipin functions as a localization signal and the presence of cardiolipin is sufficient for MgtA localization to the cell poles, its localization was analyzed in *Vibrio cholerae*. *V. cholerae* is a Gram-negative bacterium with a similar membrane composition as *E. coli* [44]. However, it does not encode an endogenous MgtA homolog. Fluorescently-tagged MgtA did not localize to *V. cholerae* cell poles but distributed equally along the entire cell membrane (Fig. 6 C, D). To verify that the fluorescent signal is constituted by Clover-MgtA, a western blot directed against GFP investigating the expression of Clover-MgtA in *E. coli* and *V. cholerae* was performed. This control revealed that the fluorescence mainly derives from full-length Clover-MgtA in both bacterial strains and degradation products or free GFP do not contribute to the fluorescent signal (Supplementary Fig. 4). In summary, these results indicate that MgtA is localized to bacterial cell poles through an unknown mechanism, which is, at least not solely, dependent on CL.

4. Discussion

Recent research has shown the importance of lipids for membrane protein function, affecting protein activity, stability, localization, and oligomerization [45]. However, one must distinguish effects through site-specific lipid-protein interactions from effects mediated through chemical and physical properties of the bilayer, e.g., membrane fluidity, tension and thickness or interfacial curvature [45]. Studies of lipid-protein interactions have long focused on different lipid classes, varying in their hydrophobic head group. Only recently, the high selectivity of proteins binding only to specific lipids with defined hydrophobic fatty acid tails has been detected.

In our work, we investigated lipid-membrane protein interactions of bacterial magnesium transporter MgtA and its highly specific binding of cardiolipin. We identified high specificity of MgtA for two cardiolipin species, CL 18:1 and 16:0. They are essential for enzymatic activity and thermal stabilization of MgtA. Further, native MS revealed two specific cardiolipin binding sites. These results highlight, for the first time, positive cooperative binding of two different species of the same lipid type, leading to an activating effect on protein activity. However, as
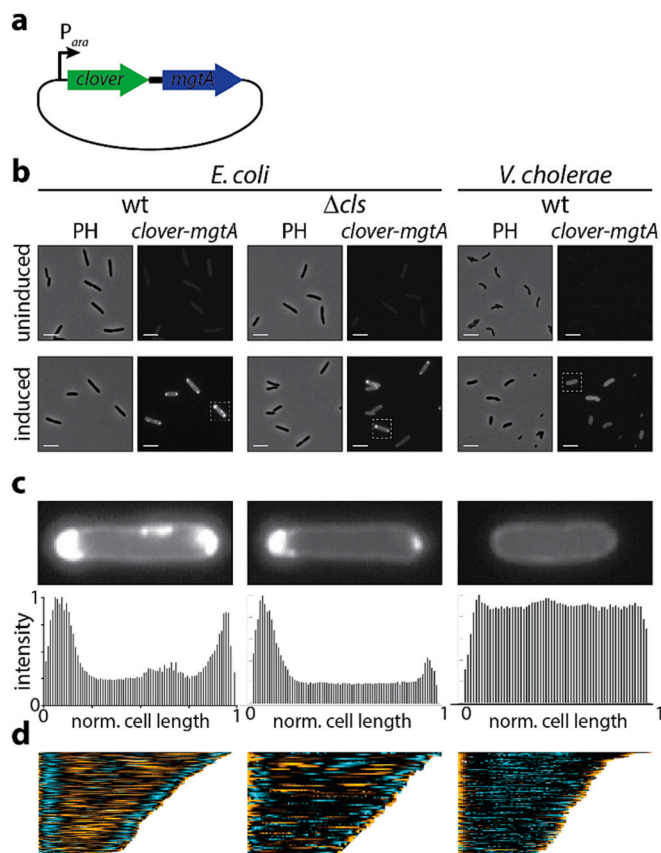
Fig. 6. MgtA localization to the pole is not solely cardiolipin-dependent. To assess whether cardiolipin functions as the main signal for polar MgtA localization in *E. coli*, in vivo imaging studies were performed using a GFP-tagged MgtA construct.
(A) Schematic representation of the Clover-MgtA expression plasmid. The expression is controlled by the arabinose-inducible P$_{ara}$ promoter.
(B) The localization of MgtA-GFP was assessed in wild-type *E. coli* strain MG1655, cardiolipin-deficient *E. coli* MG1655Δ*cls*, a knockout strain of cardiolipin synthase (Δ*cls*), and wild type *Vibrio cholerae* strain C6706. The phase contrast channel (PH) and GFP channel (Clover-MgtA) of bacteria grown in the presence of 0.2 % arabinose (induced) or in its absence (uninduced) are shown. White scale bars are 5 μm.
(C) Intensity profiles of single, representative cells (highlighted by a dotted white box in (B)). The intensities are normalized to the brightest area in each cell, respectively.
(D) Clover-MgtA localization profiles of cells sorted by their cell length. This representation approximates the localization patterns through the cell cycle, with small cells approximating newborn cells and long cells approximating cells immediately prior to division. The cell lengths are normalized to the most extended cell in each analysis, and the fluorescent intensities are normalized to the brightest area in all cells from each strain. *E. coli* MG1655 ($n = 171$ cells), *E. coli* MG1655 Δ*cls* ($n = 75$ cells), and *V. cholerae* C6706 ($n = 125$ cells).

solely CL 18:1 mediated MgtA thermal stabilization, differences in the interaction between MgtA and both CL species and, therefore, potentially different roles of both lipid species for MgtA function can be hypothesized. As native MS revealed two cardiolipin binding sites and CL 18:1 has been shown to affect thermal stability, one can hypothesize that both binding sites are preferentially occupied by CL 18:1, leading to MgtA stabilization (Fig. 7). CL 16:0 plays an essential role during MgtA ATPase activity in combination with CL 18:1. As activity assays are performed in a large excess of cardiolipin, CL 16:0 might not interact directly with MgtA but play an unknown role in the protein-lipid bilayer environment. However, this is purely speculative, and the interaction between MgtA and both CL species requires further investigation.

Interestingly, *E. coli* membranes contain a large variety of
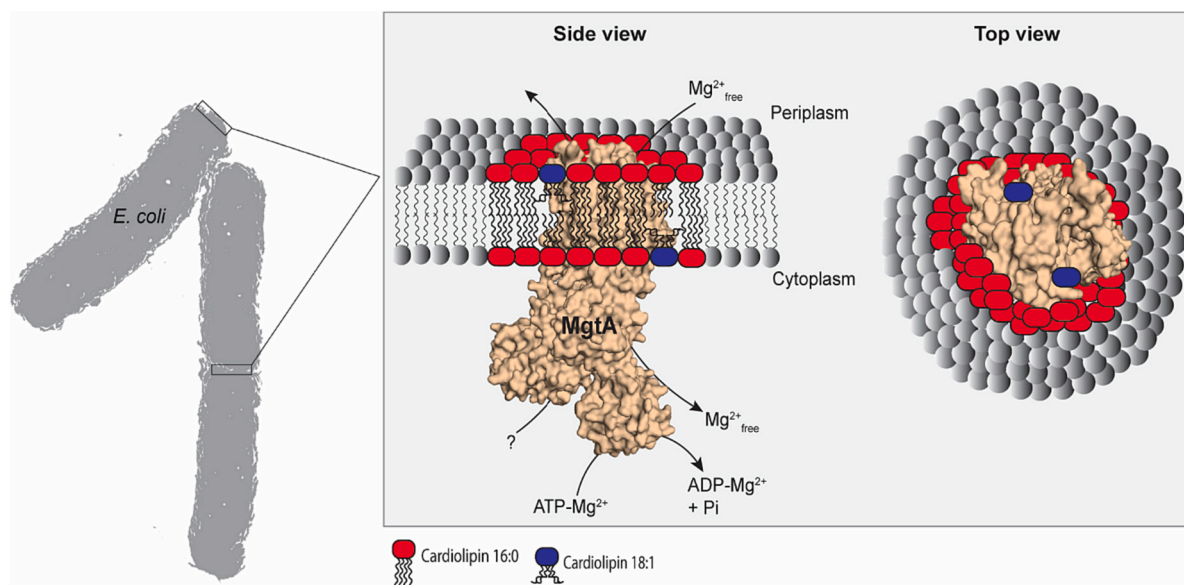
Fig. 7. Model of cardiolipin interaction with MgtA.

MgtA protein localizes in the inner membrane at the *E. coli* cell poles, which represent cardiolipin-rich regions. Association of MgtA with cardiolipin is essential for MgtA activity and stability, but MgtA shows high selectivity for specific cardiolipin species. We propose particular interaction between MgtA and two CL 18:1 molecules, affecting MgtA thermal stabilization. Further, CL18:1 is required for MgtA ATPase activity. CL 16:0 is needed for maximal MgtA activation but does not affect protein stabilization significantly.

cardiolipins, with the most abundant species containing acyl chains 18:1, 16:1, and 16:0 [30]. We highlight the importance of combining specific species CL 18:1 and 16:0 for MgtA activity, as their combination with another cardiolipin type, CL 16:1, exhibited severely decreased MgtA activity levels. Although higher V_{max} and k_{cat} were determined in the presence of cardiolipin species CL 18:1 and 16:0 in equimolar amounts in comparison to *E. coli* CL, K_m values also increased. This indicates a lower affinity of MgtA to Mg^{2+}_{free} in the presence of the specific cardiolipin species. However, higher K_m values were always detected in the presence of CL 16:0 or 16:1. The more CL species with an acyl chain length of 16 were present in the lipid mixture, the higher K_m values were determined. Meanwhile, activity studies performed in the presence of CL 18:1 alone showed a K_m of 12 μM, similar to the K_m determined in the presence of *E. coli* CL (10 μM). As an anionic lipid, cardiolipin binds Mg^{2+}, and one might speculate that different cardiolipin species vary in their binding properties to Mg^{2+}. CL tends to form non-bilayer structures, which are proposed to form dynamic protein-lipid membrane domains [46]. The phase behavior of CL is dependent on divalent cations, including Mg^{2+} [47], and further, acyl chain length and composition can affect lipid phase behavior [48]. Therefore, it can be speculated that CL species investigated here exhibit small differences in their phase behavior, leading to variations in their interaction with Mg^{2+}.

Although we have shown the importance of CL 18:1 and 16:0 for MgtA activity, the interaction between MgtA and these lipids is not completely understood yet. The molecular shape of acyl chains affects lipid packing and, therefore, membrane bilayer properties [49]. Monounsaturated lipids such as CL 18:1 exhibit a kinked shape and tend to form fluid bilayers at physiological temperatures. Consequently, they exhibit higher flexibility and fluidity in comparison to lipids with saturated acyl chains [49]. P-type ATPases undergo large conformational changes during their catalytic cycle, requiring flexibility regarding their lipid environment [50]. Other members of the P-type ATPase family, including bacterial Cu^{2+} transporter CopA or heavy metal transporter ZntA, have shown higher activity levels upon increased lipid disorder and fluidity in the presence of unsaturated lipids [51,52]. Additionally, MgtA exhibited activation in the presence of CL extracted from bovine heart membranes, which contain mainly CL 18:2

[29]. In summary, a preference of MgtA for CL 18:1 as an abundant monounsaturated lipid of the *E. coli* membrane corresponds to lipid interactions detected for other P-type ATPases.

In comparison, the interplay of CL16:0 and MgtA is more elusive and needs further investigation. As a lipid with saturated acyl chains, CL 16:0 exhibits different properties in comparison to monounsaturated lipids such as CL 18:1. Lipids with saturated acyl chains pack with higher densities and tend to form non-fluid gel phases [49], so one might speculate that CL 16:0 allows close packing of MgtA in lipid-detergent vesicles. In vivo, the lipid bilayer exerts lateral pressure that supports structural integrity. However, during the purification process, the detergent solubilization decreases lateral pressure and likely increases the conformational freedom of the protein [53]. Enzymatic assays were not performed in liposomes but instead in detergent-lipid micelles. Therefore, tighter packing of CL 16:0 might be beneficial for in vitro MgtA activation, but its function in vivo needs further investigation. Unfortunately, no additional saturated cardiolipin species could be included to investigate the effect of saturated lipids in MgtA-mediated ion transport, as only a limited selection of cardiolipins were commercially available at the time.

Further, cooperative binding of cardiolipin to MgtA was revealed, and the determined Hill coefficient of 2.4–3 in the presence of equimolar concentrations of CL 18:1 and 16:0 (Table 1) corresponds to the presence of two cardiolipin binding sites revealed by native MS. Allosteric modulation of protein-protein interactions by lipids has been previously described [42], with the *E. coli* ammonium channel AmtB binding two different lipid types, PE and CL [54]. Additionally, it was shown that individual lipid binding affected the allosteric interaction between AmtB and a soluble regulatory protein, GlnK. The allosteric modulation was highly selective regarding lipid head group and acyl chain composition. In both cases, it was proposed that the binding of certain lipids stabilizes a specific conformation of AmtB, which exhibits a higher binding affinity to PE or GlnK, respectively. One can speculate a similar mechanism for positive allosteric modulation of MgtA-CL binding as described for AmtB, as CL has been shown to stabilize MgtA. CL interaction at a specific binding site potentially stabilizes MgtA in a conformational state, which exhibits increased affinity for the second CL molecule.

Interestingly, other members of the P-type ATPase family have

shown high specificity towards lipids with a defined acyl chain composition. Their high lipid specificity has been linked to their requirement of high flexibility in the lipid bilayer due to the large conformational changes during the catalytic cycle [50]. SERCA adapts to membranes of different hydrophobic thicknesses by inducing local deformations, and a mismatch between the hydrophobic thickness of the bilayer and its membrane embedded part for optimal flexibility is required, with 1-Palmitoyl-2-oleoyl-sn-glycero-3-phosphocholine (16:0–18:1-PC) as the optimal lipid environment for SERCA. Shorter PC species (di-14:1-PC) were shown to surround the protein like a straitjacket, which prevented rotational and translational movement of the transmembrane helices [55]. MgtA also exhibited decreased activation in the presence of the shorter cardiolipin species CL 14:1, likely induced by decreased flexibility required for conformational changes.

It should be noted that, although we propose CL 16:0 plays a more indirect role for MgtA function in the protein-lipid bilayer environment, it cannot be excluded that the two identified cardiolipin binding sites are occupied with one from each cardiolipin species, one CL 18:1 and one CL 16:0. Small mass differences were identified between the first and second bound cardiolipin in the native MS spectrum (Fig. 1), with the second bound CL revealing a slightly higher mass (ca. $1440 +/- 125\,Da$) in comparison to the first one ($1380 +/- 200\,Da$). The calculated masses for CL 18:1, which has four identical oleic acid chains, and CL 16:0, with four palmitic acid tails, are 1501.0 Da and 1396.9 Da, respectively, making it tempting to suggest that the first binding site is occupied by CL 16:0, while CL 18:1 binds preferentially to the second site. One could speculate that each cardiolipin species could match the hydrophobic thickness of a specific conformational state of MgtA during the catalytic cycle, exhibiting different binding affinities in other states. However, native MS did not reveal changes in the cardiolipin binding of MgtA locked in different conformations in the presence of inhibitors (Supplementary Fig. 3). The resolution of the native MS experiments was too low to distinguish distinctively different cardiolipin species. Therefore, additional native MS studies with higher resolution could allow the identification of specific cardiolipin species bound to the two sites on MgtA. Further, native MS of lipid titration of CL 18:1 in the presence of CL of 16:0, and vice versa, would allow the determination of binding affinities of each cardiolipin species and could shed further light on the cooperative interaction between the lipids and the enzyme.

Other P-type ATPases also revealed site-specific lipid binding sites. For Na$^+$/K$^+$-ATPase, two distinct lipid binding sites have been detected [11]. Interestingly, distinctive properties were assigned for both sites. Lipid binding site A was connected to the stabilization of the pump, while lipid binding site B did not affect stabilization but stimulated activity. Both effects are independent. We have no indication of distinct functions associated with the identified two cardiolipin binding sites on MgtA. As the removal of cardiolipin strongly affected MgtA stability, making native MS spectrum acquisition difficult, a role of both lipid sites for MgtA stability is likely.

It should be noted that native MS was performed in DDM, whereas other studies replaced DDM with UDM, which has a higher critical micelle concentration and, therefore, allows the acquisition of the spectra at lower activation energy [11]. This might also allow obtaining spectra of less stable MgtA mutants. Although native MS measurements revealed the binding of two cardiolipin molecules, no indication of the localization of the lipid binding site on MgtA could be obtained. In future work, structural characterization of lipid-protein interaction by in silico or experimental methods, such as X-ray crystallography or cryo-EM, should be conducted to provide answers to the interaction sites and role of the lipids for MgtA function.

We also investigated co-localization of MgtA with cardiolipin at bacterial cell poles. Lipids have been linked to membrane protein localization, e.g., polar localization of osmosensory transporter ProP correlates with proportion and localization of cardiolipin and is less pronounced in *cls*$^-$ cells [28]. Therefore, cardiolipin has been proposed to promote ProP localization [28]. Previous studies also showed co-

localization of MgtA to cell poles with cardiolipin, proposing a promoting role of cardiolipin for MgtA localization [15]. Our work confirmed the polar localization of MgtA in *E. coli* wild-type strain MG1655. MgtA is also localized at the cell poles in a cardiolipin synthase knockout strain, *E. coli* MG1655Δ*clsABC*. In this mutant strain, no CL was detectable independent of the bacterial growth phase [56]. However, the total depletion of CL by genetic approaches induced increased PG concentrations at the cell poles. Since PG previously has revealed activation of MgtA, although, to a much lesser extent than CL, MgtA could exhibit some promiscuity at the relatively high levels of PG and display a pattern of cellular localization that is not influenced by depletion of CL [57]. Therefore, no conclusion on the importance of cardiolipin for MgtA localization in *E. coli* can be assumed. Interestingly, in *V. cholerae*, which contains a similar membrane composition as *E. coli*, but no homolog, MgtA did not exhibit polar localizaion, but localized over the entire cell membrane. This highlights that cardiolipin does not function as the sole signal and promoter of polar MgtA localization. Further research must be performed to identify the mechanism for MgtA localization. A previously predicted signal peptide at the N-terminus, enriched in positively charged residues and hypothesized to interact with cardiolipin, was shown not to be involved in MgtA localization at the cell poles [15], but recent results imply a role of the N-terminus as a lipid anchor for MgtA [58].

In summary, our results reveal a complex interplay between MgtA and selective cardiolipin species, affecting MgtA activity, stability, and localization. Insights obtained here contribute to our understanding of lipid specificity and lipid interaction of membrane proteins in general.

CRediT authorship contribution statement

J.W., J.P.M., S.S. conceptualized the research and provided funding. J.P.M. and F·S led the study and wrote the manuscript with J.W. and J.F. D. cloning, expression, and purification of the magnesium transporter for kinetic, thermostability, and MS analysis were performed by J.W and S.S. The kinetic and thermostability analyses were performed by J.W. and J.P.M while MS analysis and evaluation were performed by J.F.D., D.P.K., S.P.M and F.S. Cloning and imaging of *E. coli* strain MG1655 and *Vibrio cholerae* was performed by M.S. and S.A. The final version of the figures was generated by J.W., M.S., and J.F.D. All authors contributed to editing the manuscript and accept the present findings and conclusions.

Declaration of competing interest

The authors declare no Competing Financial or Non-Financial Interests.

Data availability

Data will be made available on request.

Acknowledgment

Appendix A. Supplementary data

Supplementary data to this article can be found online at https://doi.org/10.1016/j.bbamcr.2023.119614.

References

[1] D.M. Engelman, Membranes are more mosaic than fluid, Nature 438 (2005) 578–580, https://doi.org/10.1038/nature04394.

[2] G. van Meer, D.R. Voelker, G.W. Feigenson, Membrane lipids: where they are and how they behave, Nat. Rev. Mol. Cell Biol. 9 (2008) 112–124, https://doi.org/10.1038/nrm2330.

[3] V. Corradi, B.I. Sejdiu, H. Mesa-Galloso, H. Abdizadeh, S.Y. Noskov, S.J. Marrink, D.P. Tieleman, Emerging diversity in lipid-protein interactions, Chem. Rev. 119 (2019) 5775–5848, https://doi.org/10.1021/acs.chemrev.8b00451.

[4] E. Reading, A. Laganowsky, T.M. Allison, C.V. Robinson, Membrane proteins bind lipids selectively to modulate their structure and function, Protein Sci. 23 (2014) 231. ://WOS:000339545700349.

[5] A. Laganowsky, E. Reading, T.M. Allison, M.B. Ulmschneider, M.T. Degiacomi, A. J. Baldwin, C.V. Robinson, Membrane proteins bind lipids selectively to modulate their structure and function, Nature 510 (2014) 172–175, https://doi.org/10.1038/nature13419.

[6] A.G. Lee, Lipid–protein interactions in biological membranes: a structural perspective, Biochim. Biophys. Acta Biomembr. 1612 (2003) 1–40, https://doi.org/10.1016/S0005-2736(03)00056-7.

[7] I.C. Mangialavori, G. Corradi, D.E. Rinaldi, M.C. de la Fuente, H.P. Adamo, J. P. Rossi, Autoinhibition mechanism of the plasma membrane calcium pump isoforms 2 and 4 studied through lipid-protein interaction, Biochem. J. 443 (2012) 125–131, https://doi.org/10.1042/BJ20111035.

[8] F. Cornelius, M. Habeck, R. Kanai, C. Toyoshima, S.J. Karlish, General and specific lipid-protein interactions in Na,K-ATPase, Biochim. Biophys. Acta 2015 (1848) 1729–1743, https://doi.org/10.1016/j.bbamem.2015.03.012.

[9] F. Cornelius, Modulation of Na,K-ATPase and Na-ATPase activity by phospholipids and cholesterol. I. Steady-state kinetics, Biochemistry 40 (2001) 8842–8851, https://doi.org/10.1021/bi010541g.

[10] M. Habeck, E. Kapri-Pardes, M. Sharon, S.J. Karlish, Specific phospholipid binding to Na,K-ATPase at two distinct sites, Proc. Natl. Acad. Sci. U. S. A. 114 (2017) 2904–2909, https://doi.org/10.1073/pnas.1620799114.

[11] M. Habeck, E. Kapri-Pardes, M. Sharon, S.J. Karlish, Specific phospholipid binding to Na,K-ATPase at two distinct sites, Proc. Natl. Acad. Sci. U. S. A. 114 (2017) 2904–2909, https://doi.org/10.1073/pnas.1620799114.

[12] F.X. Contreras, A.M. Ernst, F. Wieland, B. Brugger, Specificity of intramembrane protein-lipid interactions, Cold Spring Harb. Perspect. Biol. 3 (2011), https://doi.org/10.1101/cshperspect.a004705.

[13] K.R. Hossain, R.J. Clarke, General and specific interactions of the phospholipid bilayer with P-type ATPases, Biophys. Rev. 11 (2019) 353–364, https://doi.org/10.1007/s12551-019-00533-2.

[14] A.C. Pohland, D. Schneider, Mg2+ homeostasis and transport in cyanobacteria - at the crossroads of bacterial and chloroplast Mg2+ import, Biol. Chem. 400 (2019) 1289–1301, https://doi.org/10.1515/hsz-2018-0476.

[15] S. Subramani, H. Perdreau-Dahl, J.P. Morth, The magnesium transporter A is activated by cardiolipin and is highly sensitive to free magnesium in vitro, Elife 5 (2016), https://doi.org/10.7554/eLife.11407.001.

[16] E.A. Groisman, K. Hollands, M.A. Kriner, E.J. Lee, S.Y. Park, M.H. Pontes, Bacterial Mg2+ homeostasis, transport, and virulence, Annu. Rev. Genet. 47 (2013) 625–646, https://doi.org/10.1146/annurev-genet-051313-051025.

[17] T.J. Bourret, L. Liu, J.A. Shaw, M. Husain, A. Vazquez-Torres, Magnesium homeostasis protects Salmonella against nitrooxidative stress, Sci. Rep. 7 (2017) 15083, https://doi.org/10.1038/s41598-017-15445-y.

[18] O. Cunrath, D. Bumann, Host resistance factor SLC11A1 restricts Salmonella growth through magnesium deprivation, Science 366 (2019) 995–999, https://doi.org/10.1126/science.aax7898.

[19] H.-J. Apell, How do P-type ATPases transport ions? Bioelechemistry 63 (2004) 149–156, https://doi.org/10.1016/j.bioelechem.2003.09.021.

[20] J.P. Morth, B.P. Pedersen, M.J. Buch-Pedersen, J.P. Andersen, B. Vilsen, M. G. Palmgren, P. Nissen, A structural overview of the plasma membrane Na$^+$,K$^+$-ATPase and H$^+$-ATPase ion pumps, Nat. Rev. Mol. Cell Biol. 12 (2011), https://doi.org/10.1038/nrm3031.

[21] D.C. Ford, G.W.P. Joshua, B.W. Wren, P.C.F. Oyston, The importance of the magnesium transporter MgtB for virulence of Yersinia pseudotuberculosis and Yersinia pestis, Microbiology (Reading) 160 (2014) 2710–2717, https://doi.org/10.1099/mic.0.080556-0.

[22] M. Park, D. Nam, D.H. Kweon, D. Shin, ATP reduction by MgtC and Mg(2+) homeostasis by MgtA and MgtB enables Salmonella to accumulate RpoS upon low cytoplasmic Mg(2+) stress, Mol. Microbiol. 110 (2018) 283–295, https://doi.org/10.1111/mmi.14105.

[23] Z. Lin, X. Cai, M. Chen, L. Ye, Y. Wu, X. Wang, Z. Lv, Y. Shang, D. Qu, Virulence and stress responses of Shigella flexneri regulated by PhoP/PhoQ, Front. Microbiol. 8 (2017) 2689, https://doi.org/10.3389/fmicb.2017.02689.

[24] Y. Chadani, T. Niwa, T. Izumi, N. Sugata, A. Nagao, T. Suzuki, S. Chiba, K. Ito, H. Taguchi, Intrinsic ribosome destabilization underlies translation and provides an organism with a strategy of environmental sensing, Mol. Cell 68 (2017) 528–539.e5, https://doi.org/10.1016/j.molcel.2017.10.020.

[25] S.-Y. Park, M.J. Cromie, E.-J. Lee, E.A. Groisman, A bacterial mRNA leader that employs different mechanisms to sense disparate intracellular signals, Cell 142 (2010) 737–748, https://doi.org/10.1016/j.cell.2010.07.046.

[26] A.R. Gall, K.A. Datsenko, N. Figueroa-Bossi, L. Bossi, I. Masuda, Y.M. Hou, L. N. Csonka, Mg2+ regulates transcription of mgtA in Salmonella typhimurium via translation of proline codons during synthesis of the MgtL peptide, Proc. Natl. Acad. Sci. U. S. A. 113 (2016) 15096–15101, https://doi.org/10.1073/pnas.1612268113.

[27] M.B. Moncrief, M.E. Maguire, Magnesium transport in prokaryotes, J. Biol. Inorg. Chem. 4 (1999) 523–527, https://doi.org/10.1007/s007750050374.

[28] T. Romantsov, S. Helbig, D.E. Culham, C. Gill, L. Stalker, J.M. Wood, Cardiolipin promotes polar localization of osmosensory transporter ProP in Escherichia coli, Mol. Microbiol. 64 (2007) 1455–1465, https://doi.org/10.1111/j.1365-2958.2007.05727.x.

[29] M. Schlame, Cardiolipin synthesis for the assembly of bacterial and mitochondrial membranes, J. Lipid Res. 49 (2008) 1607–1620, https://doi.org/10.1194/jlr.R700018-JLR200.

[30] T.A. Garrett, A.C. O'Neill, M.L. Hopson, Quantification of cardiolipin molecular species in Escherichia coli lipid extracts using liquid chromatography/electrospray ionization mass spectrometry, Rapid Commun. Mass Spectrom. 26 (2012) 2267–2274, https://doi.org/10.1002/rcm.6350.

[31] S. Subramani, J. Morth, Heterologous expression and purification of the magnesium transporter a (MgtA) in Escherichia coli, Bio-Protoc. 6 (2016), https://doi.org/10.21769/BioProtoc.2001.

[32] G.S. Waldo, B.M. Standish, J. Berendzen, T.C. Terwilliger, Rapid protein-folding assay using green fluorescent protein, Nat. Biotechnol. 17 (1999) 691–695, https://doi.org/10.1038/10904.

[33] H.S. Chung, C.R. Raetz, Interchangeable domains in the Kdo transferases of Escherichia coli and Haemophilus influenzae, Biochemistry 49 (2010) 4126–4137, https://doi.org/10.1021/bi100343e.

[34] A. Paintdakhi, B. Parry, M. Campos, I. Irnov, J. Elf, I. Surovtsev, C. Jacobs-Wagner, Oufti: an integrated software package for high-accuracy, high-throughput quantitative microscopy analysis, Mol. Microbiol. 99 (2016) 767–777, https://doi.org/10.1111/mmi.13264.

[35] A. Konijnenberg, J.F. van Dyck, L.L. Kailing, F. Sobott, Extending native mass spectrometry approaches to integral membrane proteins, Biol. Chem. 396 (2015) 991–1002, https://doi.org/10.1515/hsz-2015-0136.

[36] J.F. van Dyck, A. Konijnenberg, F. Sobott, Native mass spectrometry for the characterization of structure and interactions of membrane proteins, Methods Mol. Biol. 1635 (2017) 205–232, https://doi.org/10.1007/978-1-4939-7151-0_11.

[37] J.P. Morth, B.P. Pedersen, M.S. Toustrup-Jensen, T.L.-M. Sørensen, J. Petersen, J. P. Andersen, B. Vilsen, P. Nissen, Crystal structure of the sodium-potassium pump, Nature 450 (2007), https://doi.org/10.1038/nature06419.

[38] K. Abe, K. Tani, T. Nishizawa, Y. Fujiyoshi, Inter-subunit interaction of gastric H+, K+-ATPase prevents reverse reaction of the transport cycle, EMBO J. 28 (2009) 1637–1643, https://doi.org/10.1038/emboj.2009.102.

[39] H. Nakanishi, K. Hayashida, T. Nishizawa, A. Oshima, K. Abe, Cryo-EM of the ATP11C flippase reconstituted in Nanodiscs shows a distended phospholipid bilayer inner membrane around transmembrane helix 2, J. Biol. Chem. 298 (2022), 101498, https://doi.org/10.1016/j.jbc.2021.101498.

[40] K.E. Neet, Cooperativity in enzyme function: equilibrium and kinetic aspects, Methods Enzymol. 249 (1995) 519–567, https://doi.org/10.1016/0076-6879(95)49048-5.

[41] S.J. Edelstein, N. Le Novere, Cooperativity of allosteric receptors, J. Mol. Biol. 425 (2013) 1424–1432, https://doi.org/10.1016/j.jmb.2013.03.011.

[42] J.W. Patrick, C.D. Boone, W. Liu, G.M. Conover, Y. Liu, X. Cong, A. Laganowsky, Allostery revealed within lipid binding events to membrane proteins, Proc. Natl. Acad. Sci. U. S. A. 115 (2018) 2976–2981, https://doi.org/10.1073/pnas.1719813115.

[43] B. Miroux, J.E. Walker, Over-production of proteins in Escherichia coli: mutant hosts that allow synthesis of some membrane proteins and globular proteins at high levels, J. Mol. Biol. 260 (1996) 289–298, https://doi.org/10.1006/jmbi.1996.0399.

[44] D.K. Giles, J.V. Hankins, Z. Guan, M.S. Trent, Remodelling of the Vibrio cholerae membrane by incorporation of exogenous fatty acids from host and aquatic environments, Mol. Microbiol. 79 (2011) 716–728, https://doi.org/10.1111/j.1365-2958.2010.07476.x.

[45] V. Corradi, E. Mendez-Villuendas, H.I. Ingolfsson, R.X. Gu, I. Siuda, M.N. Melo, A. Moussatova, L.J. DeGagne, B.I. Sejdiu, G. Singh, T.A. Wassenaar, K. Delgado Magnero, S.J. Marrink, D.P. Tieleman, Lipid-protein interactions are unique fingerprints for membrane proteins, ACS Cent. Sci. 4 (2018) 709–717, https://doi.org/10.1021/acscentsci.8b00143.

[46] E. Mileykovskaya, W. Dowhan, Cardiolipin membrane domains in prokaryotes and eukaryotes, Biochim. Biophys. Acta 1788 (2009) 2084–2091, https://doi.org/10.1016/j.bbamem.2009.04.003.

[47] W.J. Vail, J.G. Stollery, Phase changes of cardiolipin vesicles mediated by divalent cations, Biochim. Biophys. Acta 551 (1979) 74–84, https://doi.org/10.1016/0005-2736(79)90354-7.

[48] M.B. Sankaram, G.L. Powell, D. Marsh, Effect of acyl chain composition on salt-induced lamellar to inverted hexagonal phase transitions in cardiolipin, Biochim. Biophys. Acta 980 (1989) 389–392, https://doi.org/10.1016/0005-2736(89)90331-3.

[49] R. Ernst, C.S. Ejsing, B. Antonny, Homeoviscous adaptation and the regulation of membrane lipids, J. Mol. Biol. 428 (2016) 4776–4791, https://doi.org/10.1016/j.jmb.2016.08.013.

[50] L. Thogersen, P. Nissen, Flexible P-type ATPases interacting with the membrane, Curr. Opin. Struct. Biol. 22 (2012) 491–499, https://doi.org/10.1016/j.sbi.2012.05.009.

[51] J. Zimmer, D.A. Doyle, Phospholipid requirement and pH optimum for the in vitro enzymatic activity of the E. coli P-type ATPase ZntA, Biochim. Biophys. Acta 1758 (2006) 645–652, https://doi.org/10.1016/j.bbamem.2006.04.008.

[52] H.E. Autzen, H. Koldso, P.J. Stansfeld, P. Gourdon, M.S.P. Sansom, P. Nissen, Interactions of a bacterial cu(I)-ATPase with a complex lipid environment,

Biochemistry 57 (2018) 4063–4073, https://doi.org/10.1021/acs.biochem.8b00326.

[53] H. Palsdottir, C. Hunte, Lipids in membrane protein structures, Biochim. Biophys. Acta 1666 (2004) 2–18, https://doi.org/10.1016/j.bbamem.2004.06.012.

[54] X. Cong, Y. Liu, W. Liu, X. Liang, A. Laganowsky, Allosteric modulation of protein-protein interactions by individual lipid binding events, Nat. Commun. 8 (2017) 2203, https://doi.org/10.1038/s41467-017-02397-0.

[55] Y. Sonntag, M. Musgaard, C. Olesen, B. Schiott, J.V. Moller, P. Nissen, L. Thogersen, Mutual adaptation of a membrane protein and its lipid bilayer during conformational changes, Nat. Commun. 2 (2011) 304, https://doi.org/10.1038/ncomms1307.

[56] S. Ryabichko, V.M. Ferreira, H. Vitrac, R. Kiyamova, W. Dowhan, M. Bogdanov, Cardiolipin is required in vivo for the stability of bacterial translocon and optimal membrane protein translocation and insertion, Sci. Rep. 10 (2020) 6296, https://doi.org/10.1038/s41598-020-63280-5.

[57] P.M. Oliver, J.A. Crooks, M. Leidl, E.J. Yoon, A. Saghatelian, D.B. Weibel, Localization of anionic phospholipids in Escherichia coli cells, J. Bacteriol. 196 (2014) 3386–3398, https://doi.org/10.1128/JB.01877-14.

[58] S. Jephthah, L.K. Mansson, D. Belic, J.P. Morth, M. Skepo, Physicochemical characterisation of KEIF-the intrinsically disordered N-terminal region of magnesium transporter a, Biomolecules 10 (2020), https://doi.org/10.3390/biom10040623.